Restriction/Classification Cancelled

CONFIDENTIAL

Copy 1
RM E54L16

NACA RM E54L16

CLASSIFICATION CANCELLED
Authority NASA PUBLICATIONS ANNOUNCEMENTS NO. 29
Date 9/29/60 By

APR 12 1956

Restriction/Classification Cancelled

NACA

RESEARCH MEMORANDUM

COMPONENT PERFORMANCE INVESTIGATION OF J71 EXPERIMENTAL TURBINE

II - INTERNAL-FLOW CONDITIONS WITH 97-PERCENT-DESIGN STATOR AREAS

By John J. Rebeske, Jr., and Donald A. Petrash

Lewis Flight Propulsion Laboratory
Cleveland, Ohio

Restriction/
Classification Cancelled

This material contains information affecting the national defense of the United States within the meaning of the espionage laws, Title 18, U.S.C., Secs. 793 and 794, the transmission or revelation of which in any manner to an unauthorized person is prohibited by law.

NATIONAL ADVISORY COMMITTEE
FOR AERONAUTICS
WASHINGTON
April 11, 1956

FILE COPY
To be returned to the files of the National Advisory Committee for Aeronautics Washington, D.C.

CONFIDENTIAL

CLASSIFICATION CANCELLED
Authority NASA PUBLICATIONS ANNOUNCEMENTS NO.

NASA Technical Library
3 1176 01435 7793

 [redacted]

UNCLASSIFIED

NATIONAL ADVISORY COMMITTEE FOR AERONAUTICS

RESEARCH MEMORANDUM

COMPONENT PERFORMANCE INVESTIGATION OF J71 EXPERIMENTAL TURBINE

II - INTERNAL-FLOW CONDITIONS WITH 97-PERCENT-DESIGN STATOR AREAS

By John J. Rebeske, Jr., and Donald A. Petrash

3570

SUMMARY

An experimental investigation of the internal-flow conditions of a J71 experimental turbine equipped with 97-percent-design stator areas was conducted at equivalent design speed and near equivalent design work. The results of the investigation indicate that the stage work distribution closely approximates design, the actual distribution being 44.1, 33.4, and 22.5 percent for the first, second, and third stages, respectively. The first-, second-, and third-stage efficiencies were 0.894, 0.858, and 0.792, respectively.

The first and second stages exhibited loss regions near the hub and tip at the rotor blade outlets. The hub loss region is attributed to stator secondary flows, and a contributing factor to the tip loss region may be the high design diffusion on the rotor blade suction surface near the tip. The loss in the third stage is appreciably greater than that in the first or second stage. The fact that the third rotor is unshrouded and has a nominal tip clearance of 0.120 inch may contribute to the higher loss in the tip region of the third stage.

INTRODUCTION

As part of a general investigation of high-work-output, low-speed multistage turbines at the NACA Lewis laboratory, the internal-flow conditions of a J71 experimental three-stage turbine have been experimentally determined at design equivalent speed and at approximate design equivalent work and pressure ratio. This particular three-stage turbine configuration was equipped with first-, second-, and third-stage stators with areas of 97 percent of design. The over-all performance of this turbine is presented in reference 1. The turbine exhibited reasonably good over-all performance, the efficiency being 0.877 at design equivalent speed and work output.

[redacted]

UNCLASSIFIED

In order to obtain additional and more detailed information on the performance of the turbine, interstage instrumentation was installed to determine individual stage performance, radial distribution of flow angles and velocities, and loss areas in the turbine. Because of the complex nature of the instrumentation required to measure the internal flow conditions in a multistage turbine, the measurements were limited to radial surveys at one or two circumferential positions between blade rows. Although it is recognized that large circumferential flow variations may exist downstream of blade rows (refs. 2 and 3), it is believed that the instrumentation downstream of the rotors was adequate to reveal any major loss region in the turbine, because the average of two or more circumferential positions was used. Even so, the measurements are not considered quantitative and are interpreted as indicating the trends of comparative performance of a particular blade row or turbine stage.

SYMBOLS

The following symbols are used in this report:

A	annular area, sq ft
c	actual blade chord, ft
D	diffusion factor, $\frac{W_{max} - W_o}{W_{max}}$
g	acceleration due to gravity, 32.174 ft/sec^2
p	pressure, lb/sq ft
R	gas constant, 53.4 ft-lb/(lb)($^{\circ}$R)
r	radius, ft
s	blade spacing, ft
T	temperature, $^{\circ}$R
U	wheel speed, ft/sec
V	absolute gas velocity, ft/sec
W	relative gas velocity, ft/sec
α	absolute flow angle (measured from axial direction), deg
β	relative flow angle (measured from axial direction), deg

γ ratio of specific heats

η adiabatic efficiency

ρ gas density, lb/cu ft

σ solidity, ratio of actual blade chord to blade spacing, c/s

ω angular velocity, radians/sec

$\bar{\omega}$ loss coefficient

Subscripts:

av mass-averaged value

i inlet

max maximum

o outlet

u tangential

x axial

$\left.\begin{matrix}0,1,2,3\\4,5,6,7\end{matrix}\right\}$ measuring stations (see fig. 1)

Superscripts:

' stagnation or total state

" relative stagnation or total state

METHODS AND PROCEDURE

Instrumentation

The experimental test installation, the method of power absorption, and the turbine are as described in reference 1. Additional interstage instrumentation used for the present investigation consisted of movable, unshielded total-pressure probes with provision for angle measurement. These probes were mounted in remotely controlled actuators and were used to measure the radial variations of total pressure and angle at the measuring stations indicated in figure 1. Photographs of typical total-pressure and thermocouple probes are presented in figure 2. Total temperatures were measured by two fixed calibrated spike-type thermocouple

3570

CC-1 back

rakes. Each rake consisted of five thermocouples located radially at the alternate area centers of ten equal annular areas, and were located at different circumferential positions as indicated in figure 1.

Static pressure at any radius was determined by assuming a linear radial variation between the average of the value measured by wall static taps on the inner and outer shrouds at a given measuring station. At stations 3 and 5, however, the static pressure was assumed constant at the value indicated by the wall static taps on the inner shroud. This assumption was made because the measured static-pressure ratios across the rotor hubs were reasonably close to values calculated from the design velocity diagram, and the indicated wall static pressures on the outer shroud were lower than the hub value, a condition that is in direct contradiction to the considerations of simple radial equilibrium. It is believed that these tip values reflected a local flow condition (perhaps the flow around the sharp corners of the outer shrouds, see fig. 1) and as such would be meaningless in calculating the mainstream flow velocities.

3570

Test Conditions and Procedure

The survey data were obtained by operating the turbine at the equivalent design speed of 3028 rpm, an equivalent work output of 31.1 Btu per pound, and a rating pressure ratio $p_1'/p_{x,7}'$ of 3.37. It is felt that this value of equivalent work output is sufficiently close to the equivalent design value of 32.4 Btu per pound that the actual internal-flow conditions may be evaluated in terms of the design flow conditions for the turbine. The inlet stagnation pressure and temperature at station 0 (fig. 1) were nominally 35 inches of mercury absolute and 700° R. Total-pressure and angle surveys were taken at stations 1 to 7 at fifteen radial positions corresponding to 2.5, 5, 10, 15, 20, 30, 40, 50, 60, 70, 80, 85, 90, 95, and 97.5 percent of annular area. Indicated total-temperature readings were obtained at stations 3, 5, and 7 from the fixed thermocouple rakes whose thermocouples were located at radial positions corresponding to 5, 15, 25, 35, 45, 55, 65, 75, 85, and 95 percent of annular area.

Internal-Flow Calculations

Equivalent stage work. - The local work output of a stage is expressed as an equivalent stage temperature drop:

$$\frac{\Delta T'}{T'} = 1 - \frac{T_o'}{T_i'} \tag{1}$$

where T_o' and T_i' are local values evaluated along an assumed streamline passing through a given percentage of annular area at any given measuring station.

Stage and over-all efficiencies. - The local values of turbine stage and over-all adiabatic efficiencies were calculated from

$$\eta_{i-o} = \frac{1 - \frac{T_o'}{T_i'}}{1 - \left(\frac{p_o'}{p_i'}\right)^{\frac{\gamma-1}{\gamma}}} \tag{2}$$

3570

where the local values of both total pressures and temperatures are obtained at a given percentage of annular area.

Mass-averaged values. - Mass-averaged values of stage and over-all work and efficiency were obtained from the equation

$$(\ )_{av} = \frac{\int_0^A (\ )\rho V_x \, dA}{\int_0^A \rho V_x \, dA} \tag{3}$$

where ( ) indicates the local value of either work or efficiency obtained from equation (1) or (2), and $\rho V_x \, dA$ is the corresponding local value at either the stage or turbine outlet. A numerical integration was used to evaluate the integrals.

Velocities and flow angles. - The local values of stagnation temperature, pressure, and static pressure were used in the one-dimensional energy equation to calculate the absolute flow Mach numbers and velocities. Components of these velocities V_x and V_u were then determined from the known flow angle. These values, together with the wheel speed U, were then used to calculate the relative flow velocities, Mach numbers, and angles. As a check on the accuracy of the velocities computed from the stagnation pressure, static pressure, and angle measurements, the local value of $\Delta T'/T'$ was computed from the following equation:

$$\frac{\Delta T'}{T'} = \frac{\omega(r_i V_{u,i} - r_o V_{u,o})}{\frac{\gamma}{\gamma-1} gRT_i'} \tag{4}$$

The order of agreement between the calculated and measured values of $\Delta T'/T'$ indicates the accuracy of the flow measurements and assumptions used to calculate the flow velocities and angles.

Loss parameter. - A stage loss parameter is defined herein by the equation

$$\bar{\omega} = \frac{p_i'' - p_o''}{p_i'' - p_o} \tag{5}$$

where the relative total-pressure drop across the rotor is assumed to represent the loss across the complete stage. This assumption is made because detailed circumferential and radial surveys are necessary to define the total-pressure loss across the stators. Isentropic flow across the stators was assumed in evaluating the stage loss coefficient, because only radial surveys were made in this investigation and the total pressures measured at the rotor outlet are believed to be more representative of an average value. The loss coefficient $\bar{\omega}$ was evaluated in terms of absolute total-pressure and total-temperature ratios across the stage and flow conditions at the rotor outlet. The equations used are given in the appendix.

3570

This loss coefficient $\bar{\omega}$ was then multiplied by the cosine of the relative rotor leaving angle β_o (where β_o is evaluated from the design vector diagrams) and divided by the rotor blade solidity σ. It can be shown that, for incompressible flow,

$$\frac{\bar{\omega} \cos \beta_o}{\sigma} = \frac{\theta}{c} f(H)$$

where θ is the momentum thickness of the boundary layer and H is a form factor for the boundary layer. Unpublished data have shown that a plot of the loss function $\bar{\omega} \cos \beta_o/\sigma$ against a diffusion factor correlates a large amount of cascade and compressor blade-element data.

Diffusion factor. - A diffusion factor for the turbine rotor blades is defined as

$$D = \frac{W_{max} - W_o}{W_{max}} \tag{6}$$

where W_{max} is the maximum velocity on the suction surface of the rotor blade, and W_o is the average outlet velocity within the plane of the trailing edge.

It is believed that one of the factors affecting the momentum thickness of the boundary layer is the local rate of diffusion on the blade suction surface. However, the value of D defined previously is an average value, and reference 4 has indicated some correlation of turbine performance with diffusion defined in this manner. The values of D used were computed from the design vector diagrams and blade geometry by a stream-filament method given in reference 5.

3570

RESULTS AND DISCUSSION

The design velocity diagrams for the J71 experimental turbine are presented in figure 3, and the blade and channel shapes near the hub, mean, and tip sections in figure 4. Examination of figure 3 reveals that the Mach numbers at the inlet to each blade row are fairly conservative values, being on the order of 0.5. The turbine is designed for good reaction or accelerating flow across the rotors and stators, and the turning required in any blade row is less than 104°. The axial Mach number at the third-rotor outlet is less than 0.5, and the tangential velocity is small; so that, if the design velocities actually existed in the turbine, there would be no limiting-loading problem or excessive losses due to the kinetic energy of the outlet tangential velocity.

The design blade shape and passage layouts shown in figure 4 indicate that all blades are straight-backed, meaning there is no curvature in the blade suction surface downstream of the throat. Loading on this part of the blade is therefore minimized. Reference 6 indicates that this condition results in lower blade loss coefficients at a Mach number of 1. However, the reference also indicates that, where the flow Mach number does not exceed 0.8, there appears to be little difference in loss for either curved-back or straight-backed blades.

From this cursory study of the turbine vector diagrams and blade layouts, it appears that the turbine is conservatively designed and that reasonably good performance may be expected. The results of reference 1 indicate that the actual turbine equipped with stators whose areas were 97 percent of design did have reasonably good over-all performance.

Stage Performance

The stage performance results obtained in the present investigation are presented in figure 5, where the variations of stage work $\Delta T'/T'$ and stage efficiency η with annular area are shown, along with the over-all values. The mass-averaged values of work output for the first, second, and third stages are 0.1103, 0.0939, and 0.0696, respectively. These values compare favorably with the design values and represent 44.1, 33.4, and 22.5 percent, respectively, of the over-all turbine work output. The spanwise variation of the local stage work is fairly constant for the first and second stages, with deficiencies in the hub and tip regions of the blades. The third stage, however, exhibits large work deficiencies in the hub and tip regions of the blade.

The mass-averaged efficiencies for the first, second, and third stage are 0.894, 0.858, and 0.792, respectively. The spanwise variations of the local stage efficiencies for all three stages roughly parallel the spanwise variations of the local stage work. Low values of efficiency occur in the work-deficient regions near the hub and tip of the blades.

It may be well to note at this point that the third stage is not shrouded and that a nominal tip clearance of 0.120 inch exists under the cold-air test conditions. This may be a contributing factor to the poor tip performance observed in the third stage.

The mass-averaged value of the over-all turbine work is 0.2498, and the spanwise variation exhibits work deficiencies near the hub and tip. The mass-averaged value of over-all turbine efficiency is 0.868, which compares reasonably well with the value of 0.877 obtained in the over-all turbine performance reported in reference 1.

3570

The work deficiency and low efficiency observed near the hub for each of the three stages are probably caused by the low-momentum fluid of the stator secondary flows, which accumulates on the inner shroud. This fluid forms a vortex core and is swept by the mainstream through the rotors; and, as it passes through the rotors, it is displaced outward away from the inner shroud. This low-momentum fluid appears downstream of the rotors as a low-work-output, low-efficiency region.

The spanwise variation of the calculated values of $\Delta T'/T'$ shown in figure 5 agrees reasonably well with the measured values in the first and third stages. However, there is appreciable discrepancy between the measured and calculated values for the second stage. This discrepancy may be attributed to the location of the static-pressure taps at the outlet of the second stator. Of necessity, these taps were located within the stator blade passages slightly upstream of the trailing edge and probably indicated a lower static pressure than that which actually existed downstream of the stator blade. This would raise the indicated stator-outlet velocity and account for the higher level of the calculated $\Delta T'/T'$ over the midportion of the blade span.

Stage Flow Velocities and Angles

The radial variations of absolute and relative Mach numbers and angles at both the inlet and outlet of the three rotors are presented in figure 6. (Positive angles have tangential velocity components in the direction of the wheel speed U.) Design values obtained from the vector diagrams near the hub, mean, and tip are also shown. Figure 6(a) shows that the level of the absolute Mach numbers out of the first stator (or the absolute rotor-inlet Mach numbers) is higher than that of the design values. The corresponding relative Mach numbers at the rotor inlet are also higher, being on the order of 0.51 at the mean as compared with the design value of 0.40. The outlet relative and absolute Mach numbers are less than the design values, so that, in terms of relative Mach number, the reaction of the stage has decreased below the design value, tending toward an impulse or negative reaction condition near the hub of the blade.

The flow angle out of the first stator (fig. 6(a)) indicates about 2° or 3° of underturning over most of the blade span, with regions of severe underturning near the hub and overturning near the tip. This underturning exists even though the stator area was decreased by 3 percent from that of design, which increases the stator blade angle by approximately 1°. However, reference 1 shows that the turbine actually passed about 5 percent more mass flow than the design value. Since this greater mass flow is passing through the same annular area, it requires a higher axial component of velocity and contributes to the underturning observed over most of the blade height at the stator exit.

3570

The relative flow angle at the first-rotor inlet is less than design up to about 30 percent of the annular area and is greater than design over the remaining portion of the blade span. This results in negative angles of incidence near the hub and positive angles of incidence over the upper portion of the first-stage rotor blades, being on the order of 8° at 95-percent annular area (assuming that under design conditions the blades are oriented for zero angle of incidence). The relative angle at the rotor outlet indicates overturning near the hub and slight underturning over the remaining portion of the blade. The absolute outlet flow angle is on the order of 8° less than design, except in the hub and tip region of the blade. This represents a negative angle of incidence at the inlet to the second stator, except in a limited region near the hub of the blade.

Figure 6(b) shows that the second-stator outlet absolute Mach number and the second-rotor inlet relative Mach number are higher than the design values. This may be attributed in part to the aforementioned location of the static taps, which were slightly upstream of the stator blade trailing edges on both the inner and outer shrouds. The outlet relative and absolute Mach numbers are reasonably close to the design values, except in regions near the hub and tip of the blade. Again, in the second stage as in the first, the reaction in terms of relative Mach number change across the rotor has decreased from the design value.

The outlet absolute flow angle of the second stator (fig. 6(b)) is underturned by 3° or 4° over most of the blade span, with increased underturning near the hub and overturning near the tip. The variation of the relative angle at the second-stage rotor inlet indicates negative angles of incidence near the hub and positive values near the tip. The relative outlet flow angle is slightly less than the design value by some 3° or 4° over most of the blade span, except in the region near the hub. The absolute outlet flow angle is approximately 3° to 10° less than the design values over most of the blade span, except in a region at the hub, where the angle is approximately 8° greater than design. The corresponding angle of incidence on the third stator is then negative over most of the blade span and positive at the hub.

Figure 6(c) shows that the absolute Mach number at the stator outlet and the relative Mach number at the third-rotor inlet are higher than the design values. The outlet relative and absolute Mach numbers are less than the design values. This again reduces the reaction across the third rotor, with the hub and tip regions showing rather marked decreases in relative Mach number.

The third-stator outlet absolute flow angle (fig. 6(c)) agrees very well with the design values. The relative flow angle at the third-rotor inlet is greater than the design values over most of the blade span, representing positive angles of incidence on the third rotor of approximately 8°. The outlet relative angle indicates overturning in the hub region, then a slight underturning up to about 85 percent of the annular area, and a marked underturning in the tip region of the blade. The outlet absolute flow angle is nearly axial, except in the tip region of the blade.

In summary, figure 6 shows that, in general, the stator-outlet Mach numbers are higher than design values and the rotor-outlet Mach numbers are lower than design, a condition that decreases the reaction across the rotors and increases the reaction across the stators. Certainly a contributing factor to this condition is that the three stator areas for this particular turbine configuration were 3 percent smaller than the design areas. Regions of underturning exist at the three stator outlets near the hub, and overturning exists near the tip. The three rotors exhibited overturning near the hub. The third rotor has a region of marked underturning near the tip. The angles of incidence on the blade rows are small over the midportion of the blade spans and are somewhat larger in the hub and tip regions.

Stage Loss Function and Design Rotor Blade Diffusion

Figure 7 presents the variation with annular area of a stage loss function based on rotor blade geometry and the design value of diffusion on the suction surface of the rotor blades. The values of stage loss on the upper half of the blades progressively increase for the first, second, and third stages, and high loss regions also exist near the hub of the blades. Values of design rotor blade diffusion increase from the hub to the tip of the blades; and, in general, the magnitude of the second-stage values is greater than that of either the first or third stage.

As stated previously, the loss regions near the hub may be attributed to the low-momentum fluid of the stator secondary flows passing through the rotors. Figure 7 shows that both the loss and rotor blade diffusion increase on the upper third of the blades, which indicates that the higher values of rotor blade diffusion may be a contributing factor to the high loss near the tip of the blades. The larger magnitude of the loss in the tip region of the third stage may be due to the fact that the third rotor was unshrouded, whereas the first and second rotors were shrouded.

It should be pointed out that the values of rotor blade suction-surface diffusion are design values and do not necessarily represent the values that actually exist in the turbine. In fact, the actual values are higher than the design values, because the reaction of each rotor is lower than that of design. This would tend to increase the diffusion, because the outlet relative Mach numbers are decreased. However, all three stages correlate to the extent that high loss is present in the blade tip regions where the local design diffusion is highest.

3570

SUMMARY OF RESULTS

An investigation of the internal-flow conditions of the J71 experimental three-stage turbine equipped with 97-percent-design stator areas and operated near equivalent design conditions revealed that:

CC-2 back

1. The mass-averaged values of efficiency were as follows: for the first stage, 0.894; for the second stage, 0.858; and for the third stage, 0.792. The corresponding turbine over-all efficiency was 0.868.

2. The work division for the stages closely approached design values. The actual work values were 44.1, 33.4, and 22.5 percent for the first, second, and third stages, respectively.

3. The absolute Mach numbers at the stator outlets and the relative Mach numbers at the rotor inlets were higher than design values. The rotor-outlet relative and absolute Mach numbers were, in general, less than the design values, so that the rotor reaction is less than design and rotor blade suction-surface diffusion is greater than design.

4. High loss regions existed near the hub and tip at the outlet of each rotor blade row. Hub loss is attributed to stator secondary flow, and a contributing factor to the tip loss may be high diffusion on the rotor blades in the tip region.

5. Contributing factors to the poor performance of the third stage, especially in the tip region, may be the relatively large tip clearance (0.120 in.) and the fact that this stage is not shrouded.

Lewis Flight Propulsion Laboratory
National Advisory Committee for Aeronautics
Cleveland, Ohio, December 8, 1954

APPENDIX - DERIVATION OF STAGE LOSS COEFFICIENT IN TERMS OF ROTOR-OUTLET CONDITIONS

The stage loss coefficient is defined as

$$\bar{\omega} = \frac{p_i'' - p_o''}{p_i'' - p_o} \tag{5}$$

3570

Equation (5) may be rewritten as

$$\bar{\omega} = \frac{1 - \dfrac{p_o''}{p_i''}}{1 - \dfrac{p_o}{p_o'}\,\dfrac{p_o'}{p_o''}\,\dfrac{p_o''}{p_i''}} \tag{7}$$

Assuming that all the entropy increase across the stage occurs in the rotor, p_o''/p_i'' may be expressed as a function of the total-temperature and total-pressure ratios across the entire stage and the change in radius of the assumed streamline position at the rotor inlet and outlet at a given percentage of annular area. Thus,

$$\frac{p_o''}{p_i''} = \frac{p_o'}{p_i'}\left(\frac{T_o''}{T_i''}\,\frac{T_i'}{T_o'}\right)^{\frac{\gamma}{\gamma-1}} \tag{8}$$

The relative total-temperature ratio may be expressed as

$$\frac{T_o''}{T_i''} = \frac{1}{1 - \left(\dfrac{U_o^2 - U_i^2}{\dfrac{2\gamma}{\gamma-1}\,gRT_o''}\right)} \tag{9}$$

The pressure ratio p_o''/p_o' may be determined from

$$\frac{p_o''}{p_o'} = \left[1 - \left(\frac{2U_oV_{u,o} - U_o^2}{\dfrac{2\gamma}{\gamma-1}\,gRT_o'}\right)\right]^{\frac{\gamma}{\gamma-1}} \tag{10}$$

The pressure ratio p_o/p_o' is given by

$$\frac{p_o}{p_o'} = \left(1 - \frac{V_o^2}{\frac{2\gamma}{\gamma-1} gRT_o'}\right)^{\frac{\gamma}{\gamma-1}} \tag{11}$$

3570

Upon insertion of equations (8) to (11) in equation (7), the stage loss coefficient $\bar{\omega}$ is evaluated in terms of the measured total-temperature and total-pressure ratios across the stage, measured values of total temperature, total pressure, static pressure, and the calculated velocities at the rotor outlet.

REFERENCES

1. Schum, Harold J., and Davison, Elmer H.: Component Performance Investigation of J71 Experimental Turbine. I - Over-All Performance with 97-Percent-Design Stator Areas. NACA RM E54J15, 1956.

2. Whitney, Warren J., Buckner, Howard A., Jr., and Monroe, Daniel E.: Effect of Nozzle Secondary Flows on Turbine Performance as Indicated by Exit Surveys of a Rotor. NACA RM E54B03, 1954.

3. Wong, Robert Y., Monroe, Daniel E., and Wintucky, William T.: Investigation of the Effect of Increased Diffusion of Rotor-Blade Suction-Surface Velocity on Performance of Transonic Turbine. NACA RM E54F03, 1954.

4. Whitney, Warren J., Wong, Robert Y., and Monroe, Daniel E.: Investigation of a Transonic Turbine Designed for a Maximum Rotor-Blade Suction-Surface Relative Mach Number of 1.57. NACA RM E54G27, 1954.

5. Huppert, M. C., and MacGregor, Charles: Comparison Between Predicted and Observed Performance of Gas-Turbine Stator Blade Designed for Free-Vortex Flow. NACA TN 1810, 1949.

6. Ainley, D. G., and Mathieson, G. C. R.: An Examination of the Flow and Pressure Losses in Blade Rows of Axial Flow Turbines. Rep. No. R.86, British N.G.T.E., Mar. 1951.

3570

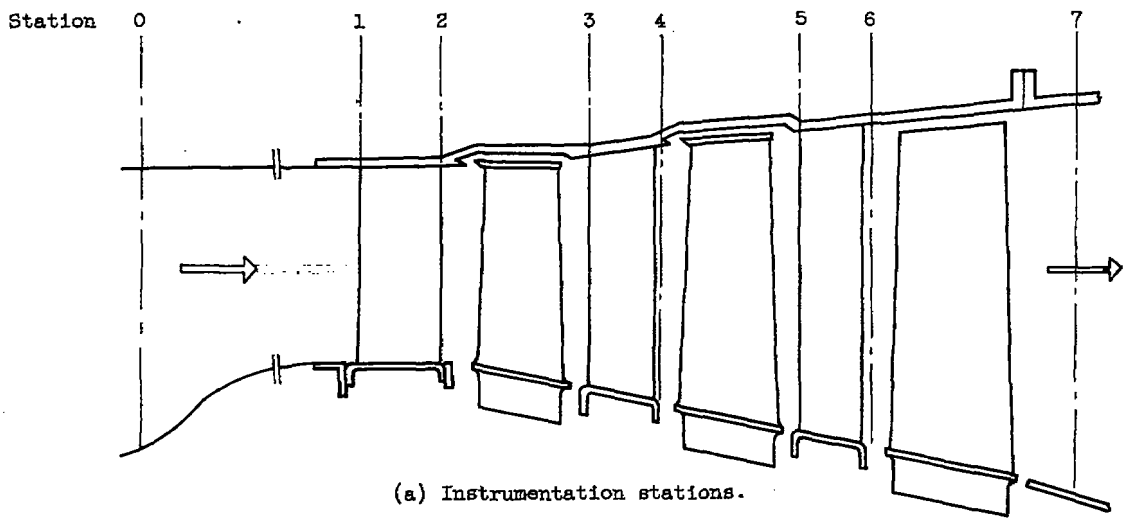

(a) Instrumentation stations.

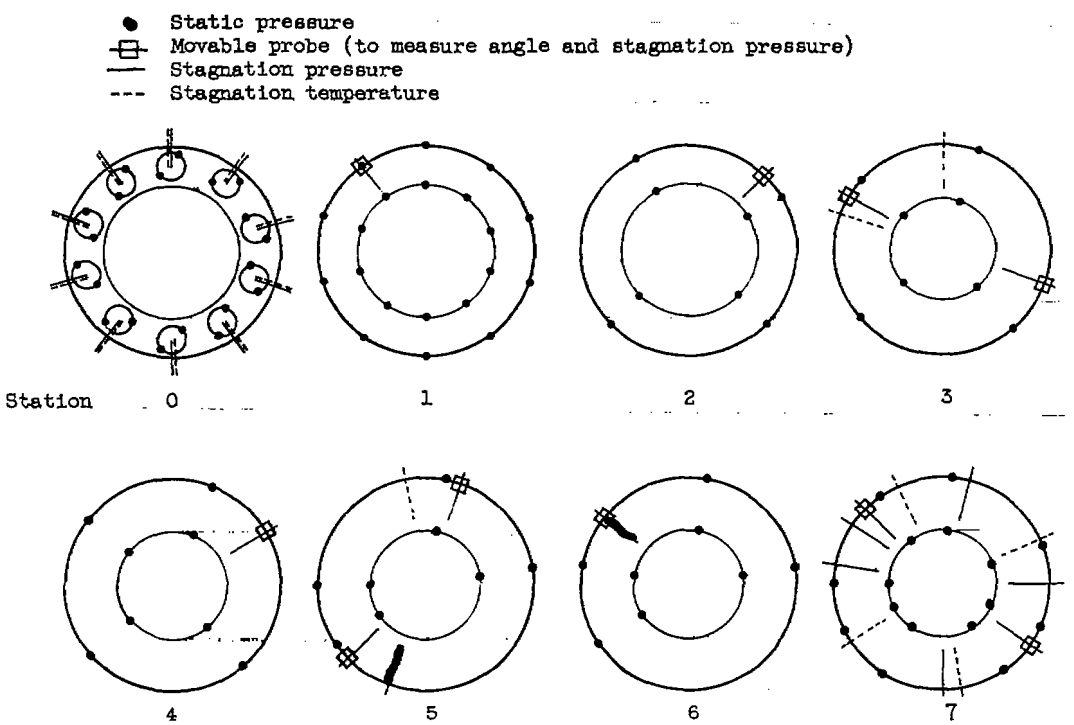

(b) Circumferential location of instruments at each station.

Figure 1. - Schematic diagram of J71 experimental turbine in radial-axial plane showing instrumentation.

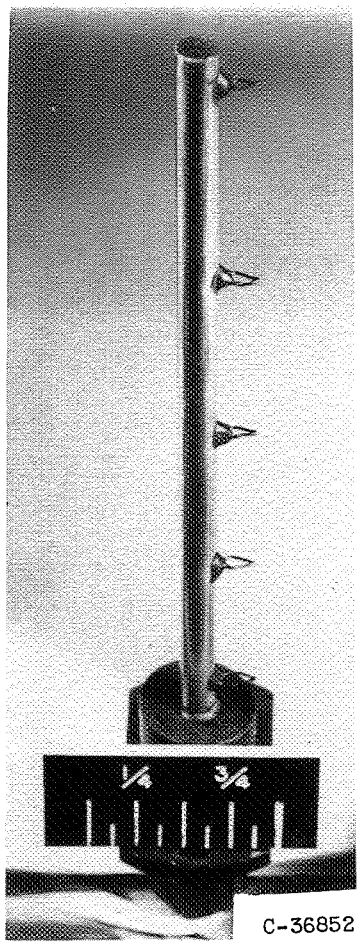

(a) Thermocouple rake.

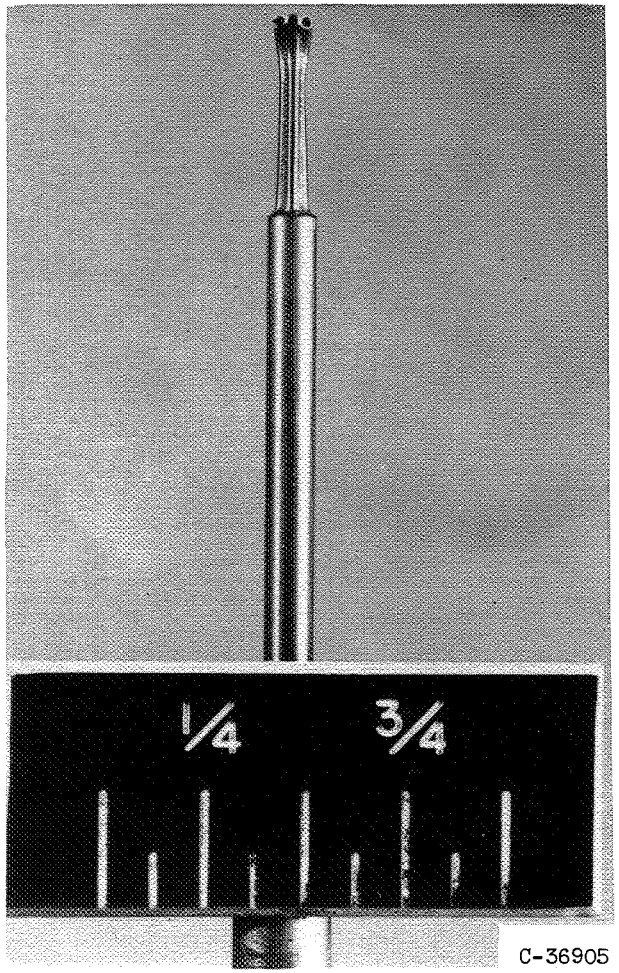

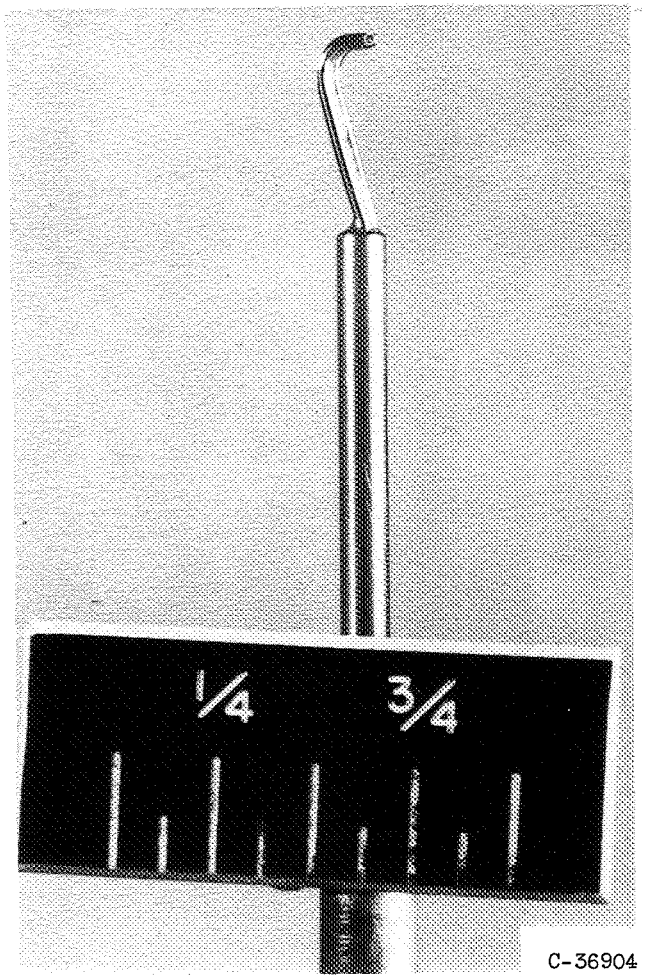

(b) Total-pressure and angle probe.

Figure 2. - Typical total-temperature rake and probe for measuring total pressure and angle.

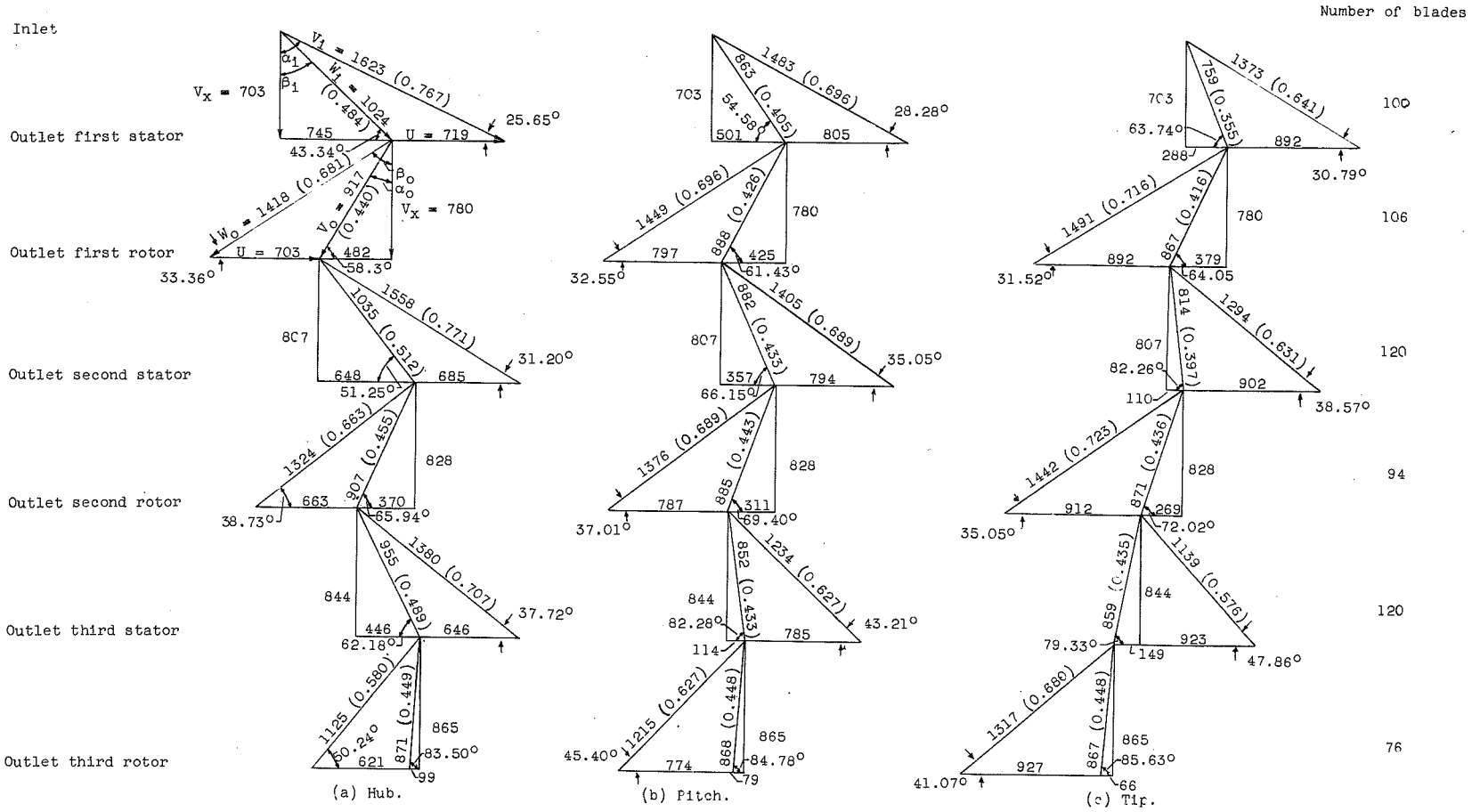

Figure 3. - Design velocity diagrams for J71 experimental turbine. (Numbers in parentheses are Mach numbers.)

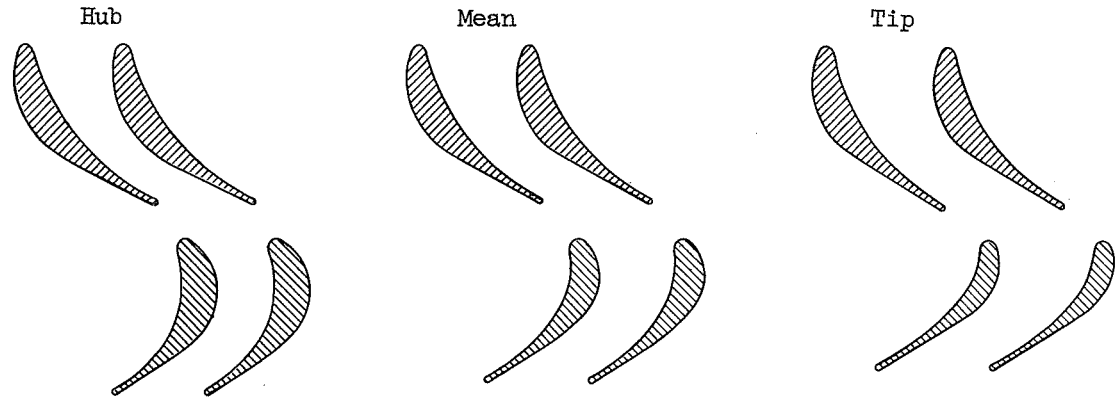

(a) First stage.

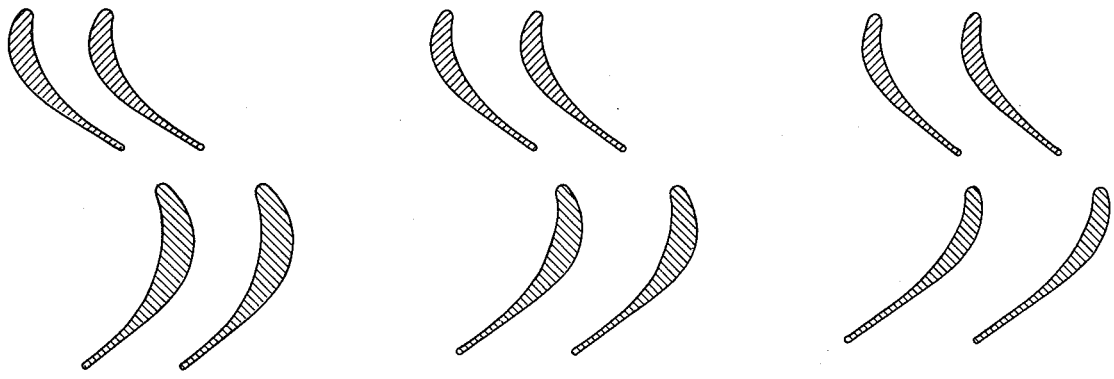

(b) Second stage.

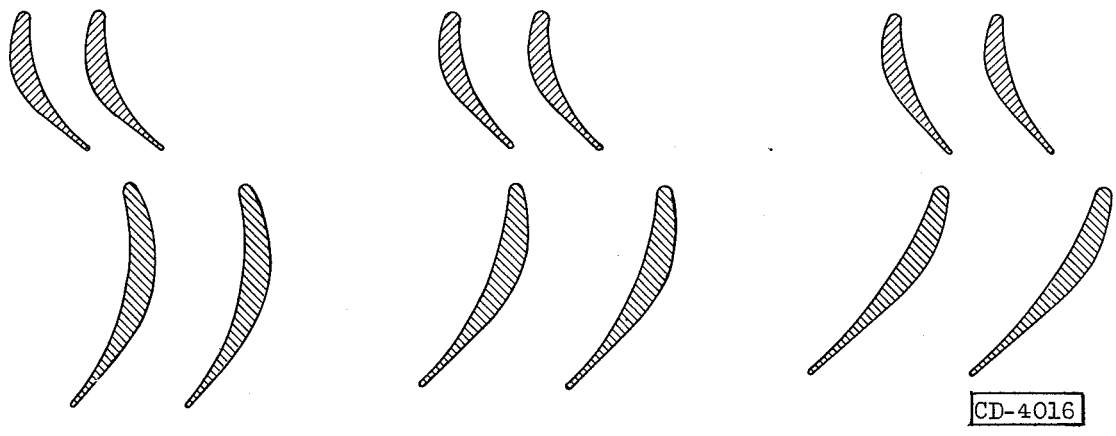

(c) Third stage.

Figure 4. - Design blade and channel shapes for J71 experimental turbine.

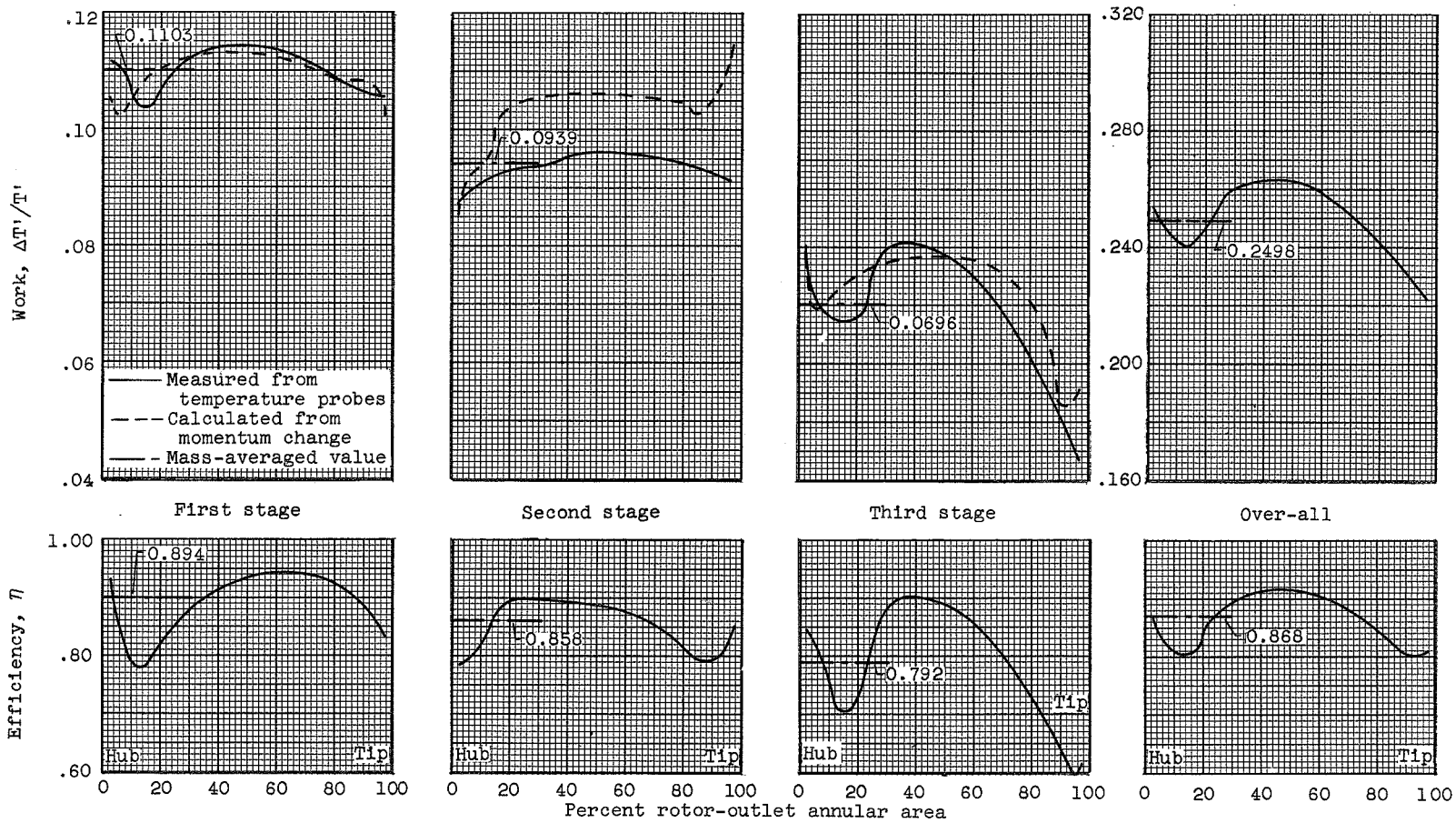

Figure 5. - Variation of stage and over-all work and efficiency of J71 experimental turbine with annular area at rotor outlets.

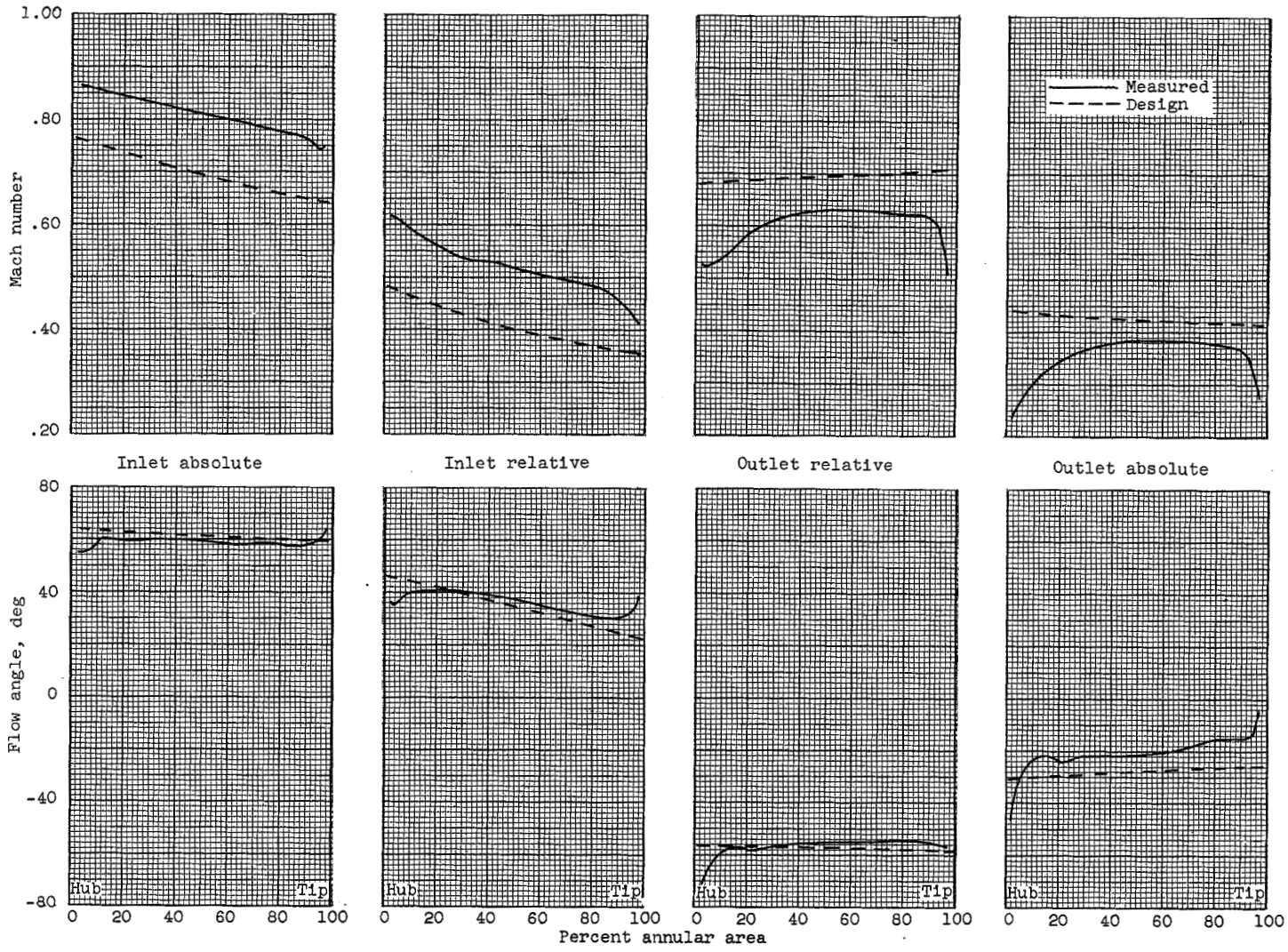

(a) First stage.

Figure 6. - Variation of absolute and relative Mach number and angle at rotor inlet and outlet with annular area.

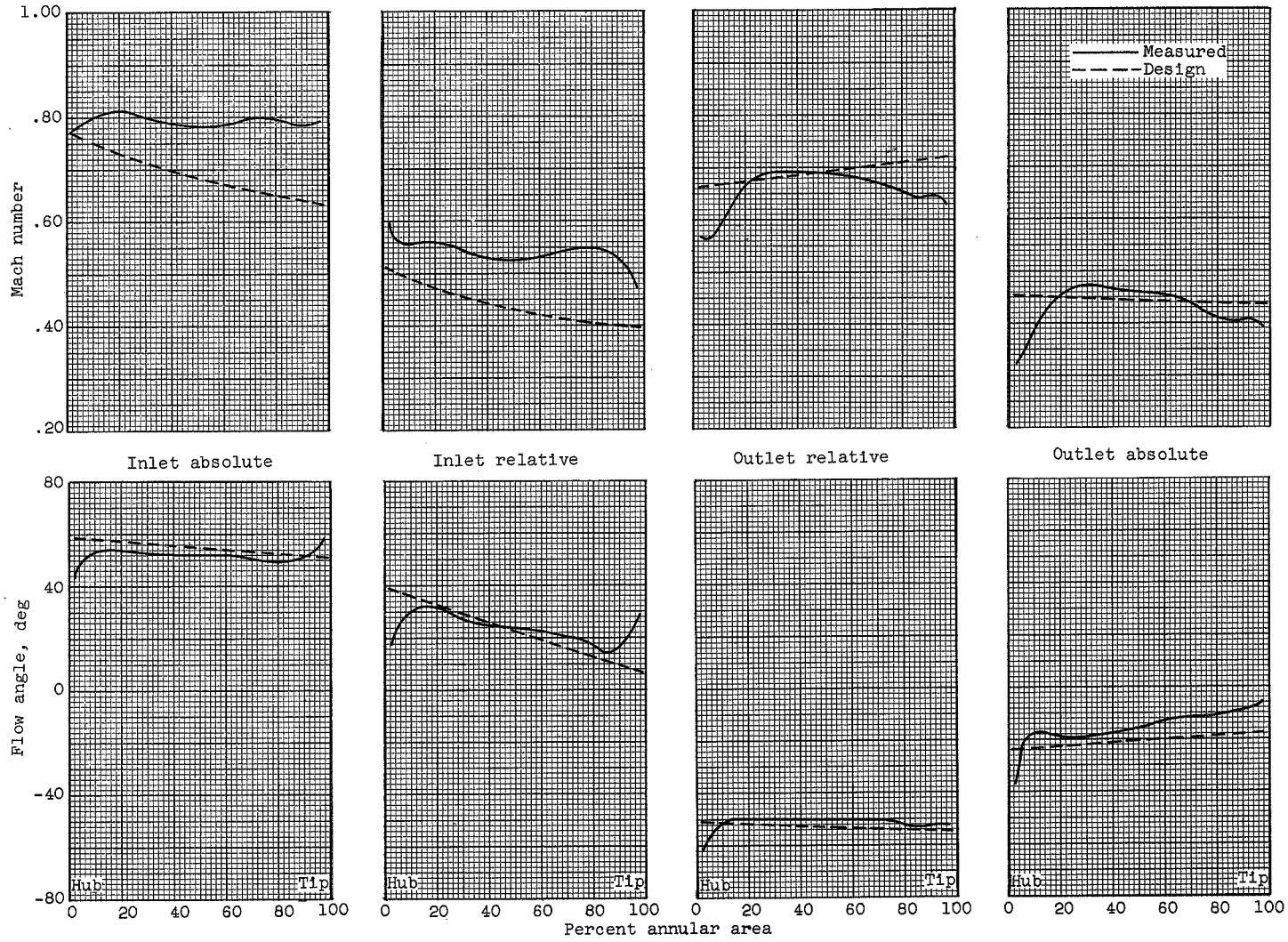

(b) Second stage.

Figure 6. - Continued. Variation of absolute and relative Mach number and angle at rotor inlet and outlet with annular area.

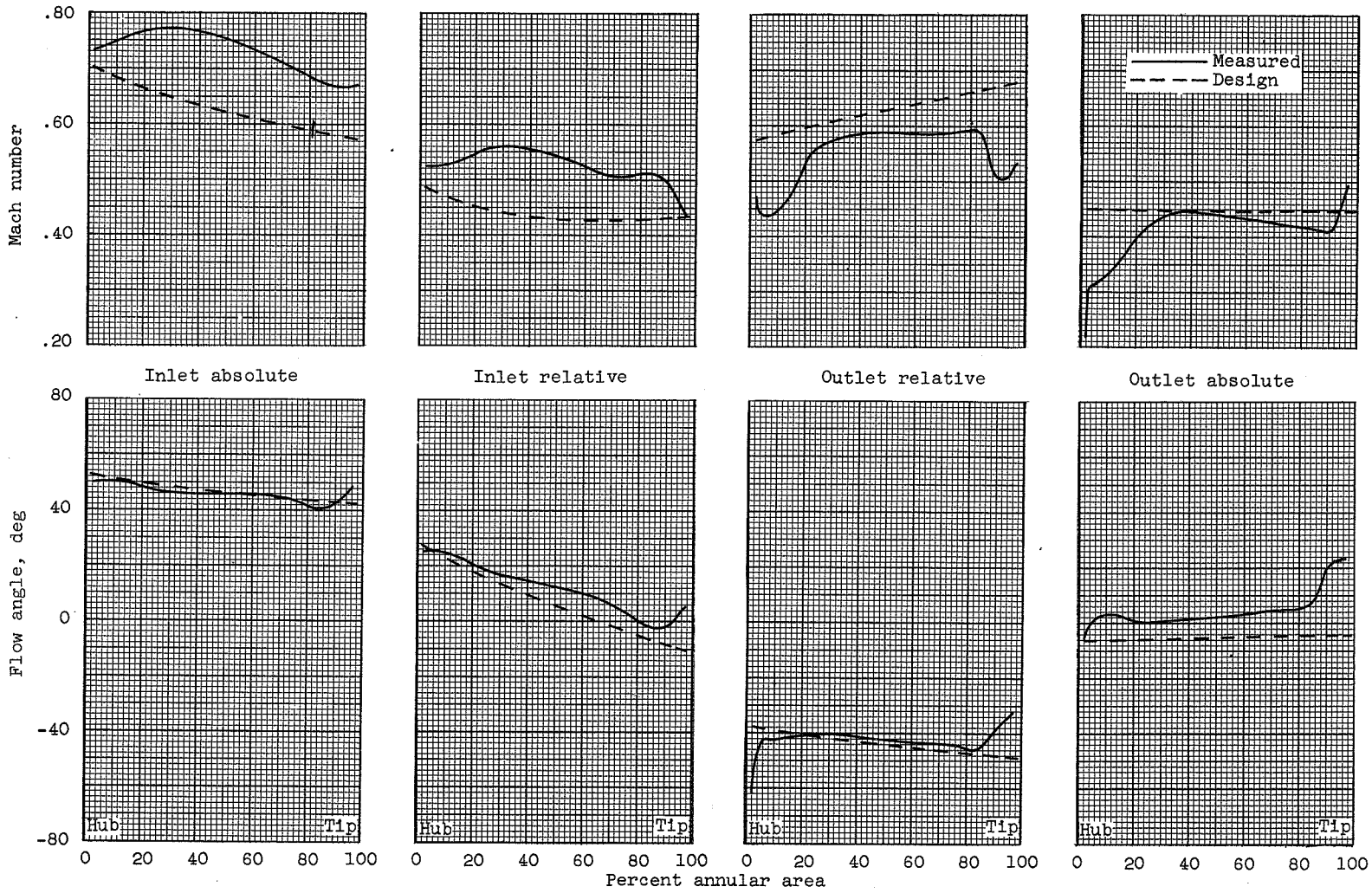

(c) Third stage.

Figure 6. - Concluded. Variation of absolute and relative Mach number and angle at rotor inlet and outlet with annular area.

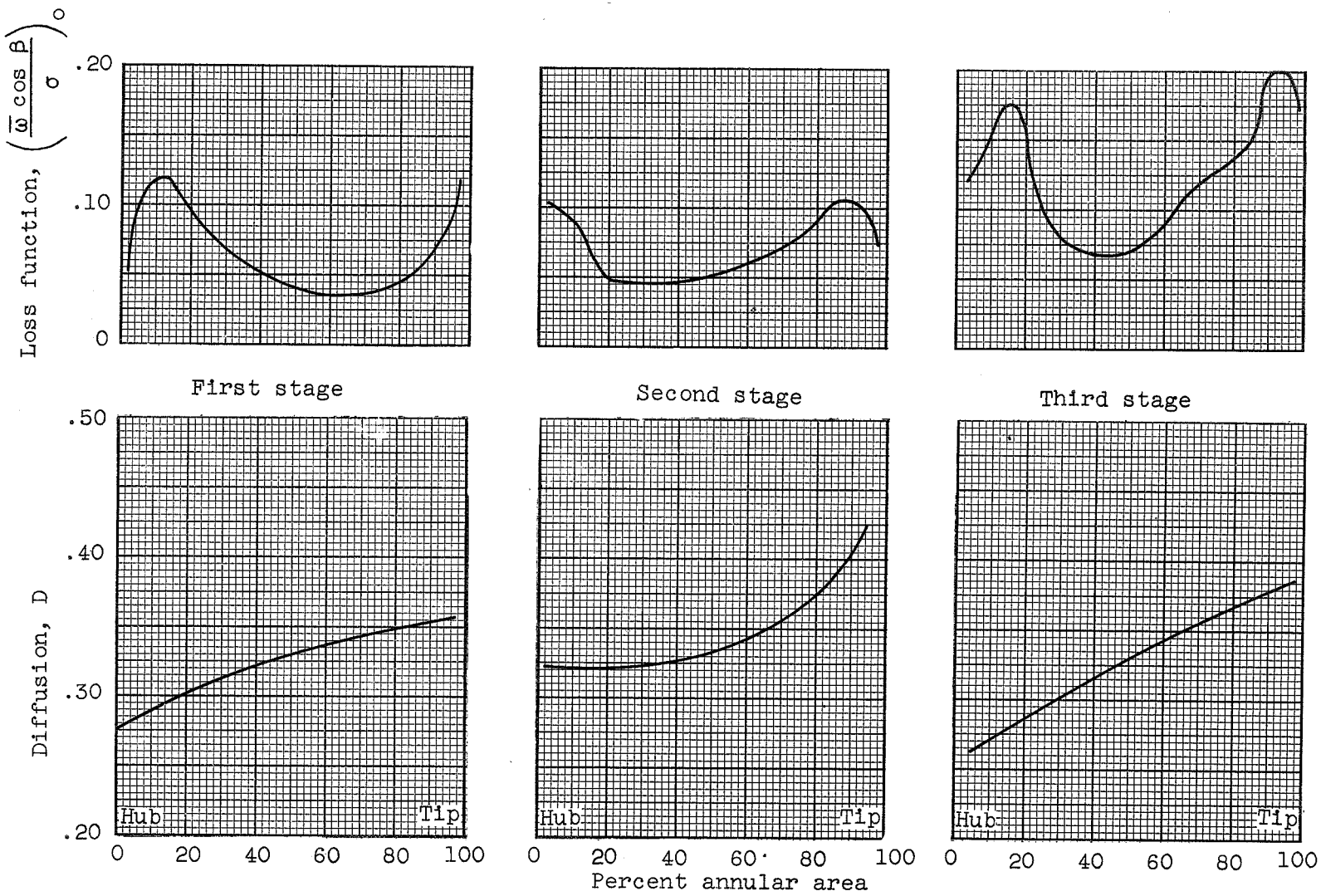

Figure 7. - Variation of loss function and design rotor blade suction-surface diffusion with annular area.

NACA - Langley Field, Va.

[redacted]

NASA Technical Library
3 1176 01435 7793

[redacted]